Available online at www.sciencedirect.com

ScienceDirect

journal homepage: www.elsevier.com/locate/he

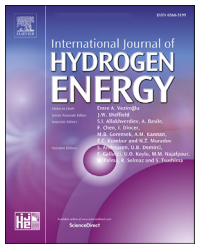

Effect of Olive Kernel thermal treatment (torrefaction *vs.* slow pyrolysis) on the physicochemical characteristics and the CO_2 or H_2O gasification performance of as-prepared biochars

Athanasios Lampropoulos [a], *Nikolaos Kaklidis* [a], *Costas Athanasiou* [b], *Miguel A. Montes-Morán* [c], *Ana Arenillas* [c], *J. Angel Menéndez* [c], *Vassilios D. Binas* [d], *Michalis Konsolakis* [e,**], *George E. Marnellos* [a,f,*]

[a] *University of Western Macedonia, Department of Mechanical Engineering, Kozani, Greece*
[b] *Democritus University of Thrace, Department of Environmental Engineering, Xanthi, Greece*
[c] *Instituto de Ciencia y Tecnología del Carbono (INCAR-CSIC), Oviedo, Spain*
[d] *Institute of Electronic Structure and Laser, Foundation for Research and Technology-Hellas (FORTH-IESL), Crete, Heraklion, Greece*
[e] *Industrial, Energy and Environmental Systems Lab (IEESL), School of Production Engineering and Management, Technical University of Crete, Chania, Crete, Greece*
[f] *Chemical Process & Energy Resources Institute, Centre for Research & Technology Hellas, Thessaloniki, Greece*

HIGHLIGHTS

- CO_2 and H_2O gasification of olive kernel and its torrefied and pyrolyzed chars was examined.
- Chars with less ordered structures, increased C, ash content and higher porosity were obtained.
- Regardless the gasification agent, an increase on gas production was observed with treatment temperature.
- A close relationship between the gasification performance and the physicochemical properties was revealed.
- The optimum behavior in terms of gas production was obtained for chars pyrolyzed at 500 and 800 °C.

ARTICLE INFO

Article history:
Received 29 July 2020
Received in revised form
19 November 2020
Accepted 25 November 2020
Available online xxx

Keywords:
Biomass
Biochar
Olive kernel
Torrefaction

ABSTRACT

The thermochemical conversion of biomass through its gasification has been widely explored during the last decades. The generated bio-syngas mixture can be directly used as fuel in thermal engines and fuel cells or as intermediate building block to produce synthetic liquid fuels and/or value added chemicals at large scales. In the present work, the effect of Greek olive kernel (OK) thermal treatment (torrefaction at 300 °C *vs.* slow pyrolysis at 500 and 800 °C) on the physicochemical characteristics and CO_2 or H_2O gasification performance of as-produced biochars is examined. Both the pristine OK sample and biochars (OK300, OK500, OK800) were fully characterized by employing a variety of physicochemical methods. The results clearly revealed the beneficial effect of thermal pretreatment on the gasification performance of as-prepared biochars. A close relationship between the physicochemical properties of fuel samples and gas production was disclosed. Carbon dioxide gasification leads mainly to CO with minor amounts of H_2 and CH_4,

* *Corresponding author*. University of Western Macedonia, Department of Mechanical Engineering, Kozani, Greece.
** *Corresponding author*.
E-mail addresses: mkonsol@pem.tuc.gr (M. Konsolakis), gmarnellos@uowm.gr, marnel@certh.gr (G.E. Marnellos).
https://doi.org/10.1016/j.ijhydene.2020.11.230

Slow pyrolysis
CO_2 and H_2O gasification

whereas steam gasification results in a mixture containing CO_2, CO, H_2 and CH_4 with a H_2/CO ratio varied between 1.3 and 2.3. The optimum gasification performance was obtained for the slowly pyrolyzed samples (OK500 and OK800), due to their higher carbon and ash content as well as to their higher porosity and less ordered structure compared to pristine (OK) and torrefied (OK300) samples.

Introduction

The world primary energy consumption is steadily increasing with an average rate of 1.6% per year in the last decade. Although there is currently an obvious trend to shift to renewables, the global energy mix is still largely depending (~85%) on fossil fuels (coal, oil and natural gas), resulting in increasing carbon emissions. Recently, the European Commission announced the European Green Deal toward a decarbonized energy future to become the world's first climate-neutral continent by 2050 with most measures being based on the deployment of renewable energy sources [1].

Biomass is a cheap and widely-distributed renewable energy source with a neutral carbon footprint. Bioenergy potential in EU is estimated to contribute with 140 Mtoe to the Gross Final Energy Consumption (GFEC) in 2020. For the target year of 2030, bioenergy could reach values between 160 and 180 Mtoe, representing a share around 14–16% of the GFEC [2]. Biomass potential for the EU was estimated by the European Environment Agency (EEA) for 2020 at 235 Mtoe including 39 Mtoe from forestry, 96 Mtoe from agriculture sector, and 100 Mtoe from waste [3]. In particular, Greece possesses a high biomass potential (3.5–5 Mtoe), with agricultural residues (e.g., olive/grapevine prunings, olive kernel) amounting at approximately 70% [4].

Despite the positive impacts of bioenergy on the way to combat climate change, biomass has several disadvantages when employed as fuel feedstock in energy conversion processes, involving its: i) lower energy density compared to fossil fuels, ii) microbiological activity which affects the lifetime of materials and processes, and iii) its high H_2O content, rendering its transfer along large distances non-financially viable [5]. To this end, different thermochemical processes have been proposed, including combustion, pyrolysis or gasification to effectively convert the energy content of biomass into power and variousbiomass-based fuels, included biofuels.

Biomass combustion, in Rankine thermal cycles, could cogenerate electricity and heat at rather low efficiencies due to the associated Carnot thermodynamic limitations [6]. Biomass pyrolysis is generally defined as the thermal decomposition of biomass organic matrix in absence of oxidizing atmospheres resulting in liquid bio-oil, solid biochar, and non-condensable gases [7]. Biomass gasification takes place at high temperatures (600–1000 °C) and atmospheric pressure by employing several gasifying agents (i.e., air or pure oxygen or/and steam or/and CO_2), resulting in a gas mixture containing mainly H_2, CO, CO_2, CH_4 and traces of light hydrocarbons. Bio-syngas from biomass gasification, can then be utilized either as fuel in Internal Combustion Engines (ICEs), gas turbines or even in high temperature solid oxide and molten carbonate fuel cells [8–12] or as raw material for the production of Fischer-Tropsch synthetic liquid fuels and value-added chemicals [13–15].

The most important parameters that affect the gasification process include the morphological and physicochemical characteristics of biomass (e.g., fixed carbon, moisture and ash content, particle size, porosity etc.), the type of gasification agent used, the operation temperature and the heating rate. Low moisture content and high ash concentration (>10%) could lead to higher syngas quality and yields [16]. In general, the endothermic steam gasification favors hydrogen production compared to other gasifying agents [17,18]. When using CO_2 as the gasifying agent, biomass gasification almost exclusively results in CO generation [19]. Although the reaction of CO_2 with carbon ($C + CO_2 \rightarrow 2CO$, reverse Boudouard reaction) is highly endothermic and thus highly energy intensive, the use of CO_2 as the gasification agent could offer an effective route for CO_2 capture and utilization (CCU) in power plants and steel industry [20]. Moreover, compared to steam, CO_2 possesses several advantages as gasification agent such as zero energy demand for vaporization while it could also tune the H_2/CO ratio in the derived bio-syngas mixtures making them suitable for different applications [21].

Biomass thermal treatment prior to gasification increases the overall performance of the gasification process by improving the fuel quality characteristics of the as-produced biochars. In particular, biochars have several advantages compared to the raw biomass, such as the low moisture and high mass-normalized energy content [7]. Many researchers have reported the advantages of torrefied and pyrolyzed biomass compared to untreated ones, comprehensively summarized in Ref. [22]. The different gasification performance between thermally upgraded and pristine biomass can be mainly attributed to the effect of pyrolysis temperature on the biochar structure [7,22–28]. Renthe et al. [29] concluded that torrefaction of Douglas fir sawdust pellet enhanced the CH_4 and H_2 yields in syngas. Bouraoui et al. [30] studied the influence of physicochemical properties of various lignocellulosic-based fuels on the CO_2 gasification performance. A close relationship between the textural and structural properties of biomass fuels and the achieved gasification rates was revealed. Similar conclusions were derived by Min et al. [28], who studied the role of pyrolysis temperature and heating rate on the gasification performance of agricultural waste chars. Char structure is a key factor that affects gasification performance.

Several researchers have also studied the effect of mineral elements on the char gasification reactivity. These mineral

Please cite this article as: Lampropoulos A et al., Effect of Olive Kernel thermal treatment (torrefaction *vs.* slow pyrolysis) on the physicochemical characteristics and the CO_2 or H_2O gasification performance of as-prepared biochars, International Journal of Hydrogen Energy, https://doi.org/10.1016/j.ijhydene.2020.11.230

elements were either presented inherently in the ash content of raw biomass or purposely added in the fuel feedstock. It has been shown that alkali (sodium, potassium) and alkaline earth (calcium, magnesium) elements are enhancing the overall gasification reactivity [31,32]. On the contrary, phosphorus and silicon compounds were found to inhibit the steam gasification performance of chars prepared from algal and lignocellulosic biomass [33].

In the present work, olive kernel (OK) from the island of Crete, Greece, was employed as raw biomass source, in order to explore the impact of pyrolysis protocol (torrefaction at 300 °C vs. slow pyrolysis at 500 °C and 800 °C) on the physicochemical properties and the CO_2 or H_2O gasification efficiency, in terms of syngas production, of as-produced biochars. Olive kernel is a by-product of olive oil production, which is an agricultural activity of great importance for the Mediterranean countries. From data received by the International Olive Oil Organization [34], in the crop year of 2018–2019, Spain, Italy, Greece and Portugal represented ca. 70% of the olive oil production globally. In specific, Greece represents the third largest olive oil industry worldwide with an annual production capacity of approximately 400,000 tons of olive kernel [35].

Due to its low cost, olive kernel has been considered as a promising biomass fuel mostly utilized for heat production in conventional burners, while its energy conversion through gasification and/or pyrolysis thermochemical processes has only scarcely studied. Most of these works focus on the gasification of pristine olive kernel using air as oxidant agent in lab scale fixed bed [36] and pilot-scale fluidized bed gasifiers [37,38], without, however, considering the impact of different gasification agents and/or the use of olive kernel chars as feedstock.

In light of above issues, and taking into account the peculiarities of olive kernel biomass compared to other lignocellulosic residues, due to its aliphatic and aromatic content, a complementary characterization study involving textural, structural and surface properties was conducted for both the pristine and thermally treated samples to gain insight into the relationship between the bio-syngas production and the physicochemical properties of investigated fuel samples. Originally, in the present study, two different gasification agents (CO_2 or H_2O) were comparatively employed towards revealing the relationship between the gas production, the gasification agent and the physicochemical properties of investigated fuel samples. To the best of our knowledge no similar study exists in the literature.

Experimental

Fuel feedstock preparation and biochars production

In the present study, Olive Kernel (OK) from Cretan olive tree cultures was selected as raw fuel. OK was first crushed to a particle size between 1 and 3 mm, using a jaw crusher and then, part of this fraction, was milled to 100–200 μm using an agate mortar (Retsch RM200) producing a large amount (ca. 70 wt%) of fines (<100 μm). In the following, the fraction between 1 and 3 mm was torrefied at 300 °C and slowly pyrolized at 500 and 800 °C under inert (N_2) atmosphere. The heat-treated samples were then also milled to 100–200 μm following a similar procedure to pristine sample.

In specific, the thermal treatment of pristine OK for obtaining the different chars was carried out in a refractory alumina boat loaded with 75 g of OK, which is placed in the middle of a horizontal refractory steel tube (Inconel®) of 8.5 cm diameter and 68 cm length. The tube was in turn placed in a horizontal electrical furnace (Carbolite GVA 12/300), keeping the sample in the stable temperature zone, and inertized with pure N_2 for 1 h at a flow of 500 cm^3/min. Then the inert flow was decreased to 250 cm^3/min and heated at a constant heating rate of 20 °C/min to the final treatment temperature (300, 500, and 800 °C), which was kept for 1 h.

The yield of the solid fraction was estimated directly by weighing the solid residue remaining after heat treatment. The liquid fraction (oil) was condensed into two serpentines (2 m length) arranged in series and ended in a bulb where the condensates were collected. The set was immersed in an ice bath. After the experiment, the yield of the liquid fraction was determined by the difference between the weight of the set filled with the condensates and the weight of the empty set. The gas fraction was indirectly determined by the difference between the initial weight of the sample and the weights of the solid and liquid fractions.

All physicochemical characterizations and gasification tests were performed using samples with fines of 100–200 μm. The pristine olive kernel sample is designated as OK. The same nomenclature along with a number corresponding to the treatment temperature is used for the heat-treated samples, i.e. OK300, OK500, and OK800.

Fuel samples characterization

The elemental analysis of feedstock samples was determined in LECO CHNS-932 (C, H, N, S) and LECO VTF-9000 (O) analyzers. Proximate analysis, in terms of volatile matter, moisture and ash contents, was performed in a LECO TGA-601 analyzer. Mineral matter composition was determined by means of X-ray fluorescence in a Bruker SRS 3000 analyzer.

The porous properties of all samples were defined by nitrogen adsorption-desorption isotherms and by the mercury porosimetry technique, performed at −196 °C, using a Micromeritics Tristar 3020 instrument and a Micromeritics AutoPore IV, respectively. Pore volume measurements by nitrogen adsorption are not precise enough for samples with large mesopores. For this reason, mercury porosimetry was used as a complementary technique to determine the volume and size of mesopores and macropores. All analyses were performed from atmospheric pressure up to 228 MPa. The surface tension and contact angle for mercury were fixed at 0.485 N/m and 130°. The volume of mesopores (V_{meso}) and macropores (V_{macro}) along with the average pore size diameter (D_p) were calculated based on Washburn's intrusion theory. It should be noted that the lowest detectable limit of the device is 5.5 nm, so that V_{meso} refers to a pore size between 5.5 and 50 nm, whereas V_{macro} refers to pores greater than 50 nm.

The High Heating Value (HHV) of the solid raw and heat treated samples was determined in a Calorimeter C4000 adiabatic from IKA®-Werke, according to the ISO 1928

Please cite this article as: Lampropoulos A et al., Effect of Olive Kernel thermal treatment (torrefaction *vs.* slow pyrolysis) on the physicochemical characteristics and the CO_2 or H_2O gasification performance of as-prepared biochars, International Journal of Hydrogen Energy, https://doi.org/10.1016/j.ijhydene.2020.11.230

standard. The Helium density, d_{He}, of the samples was measured with a Micromeritics AccuPyc 1330 pycnometer, using He as the probe gas. The samples were outgassed at 120 °C overnight prior to analysis.

The pH values of biomass fuels at the point of zero charge, pH_{pzc}, was determined by introducing 250 mg of sample into a test tube, followed by the addition of a certain volume of distilled water to modify the mass concentration of the suspension, which should be closed and under continuous stirring. Each day the pH is measured and the pH_{pzc} value is obtained from the plateau of the pH evolution profile [39].

The morphology of carbonaceous biomass fuels was examined by scanning electron microscopy (SEM) using a Quanta FEG 650 microscope, equipped with an Apollo X detector for EDX measurements. Diffractograms were recorded in a Bruker D8 powder diffractometer. It is equipped with a monochromatic CuKα X-ray source and an internal standard of Silicon powder, while the scanning rate used was 0.02° per 2 s, in the range of 5–90°.

The surface functionalities of all fuels were characterized by Raman and Fourier transform infrared (FTIR) spectroscopy. The Raman measurements were performed at room temperature using a Nicolet Almega XR Raman spectrometer with a 473 nm blue laser as an excitation source. The beam was focused on the sample through a confocal microscope equipped with a 50 × objective. The data were acquired in 400–1900 cm^{-1} range. Fourier transform infrared (FTIR) spectra were recorded on a Thermo-Electron Nicolet 6700 FT-IR optical spectrometer with a DTGS KBr detector at a resolution of 4 cm^{-1}.

Finally, the thermal behavior of the different fuel feedstock was assessed by thermogravimetric analysis in a Q5000 IR (TA Instruments) thermobalance. The mass loss profile of 15 ± 0.1 mg of sample was monitored by increasing the temperature up to 1000 °C with a heating rate of 20 °C/min, under either pure N_2 (inert) or pure CO_2 (reactive) atmosphere with a total flowrate of 20 cm^3/min. Thus, the mass loss is attributed to the single effect of temperature in the case of nitrogen flow, whereas for the experiments performed under pure CO_2 flow, its interaction with carbon further contributes to the observed weight losses.

Gasification tests

The experimental apparatus used in the present work is schematically illustrated in Fig. 1. The gasification tests of pristine olive kernel (OK) and as-produced biochars (OK300, OK500 and OK800) using either pure CO_2 or 10 vol% H_2O/He as gasifying agents was carried out in a quartz U-shape fixed-bed reactor (ID = 8 mm) under batch mode of operation and at atmospheric pressure. In each experiment, the reactor was loaded with 0.1 g of fuel with particle size of 100–200 μm. After loading the fuel sample, the reactor was placed in an electrical furnace and the temperature was gradually increased from room temperature to 300 °C, with a heating rate of 5 °C/min by flowing pure He over the sample with a total flowrate of 30 cm^3 (STP)/min. Upon reaching steady state at 300 °C, the feed was instantaneously switched from inert He to the desired gasifying agent mixture (30 cm^3 (STP)/min) and the effluents' flowrate and composition were continuously monitored in the temperature range of 300–1100 °C, by increasing the temperature with a rate of 2 °C/min.

Each experiment lasted for more than 6 h until the complete gasification of samples, leaving only ash as a residue in the reactor bed. A gas cylinder with pure CO_2 (Air Liquide) was employed to feed carbon dioxide in the lab-scale gasifier. In the case of steam gasification experiments, water vapors were fed through heated lines into the reactor by bubbling pure He (Air Liquide) as diluent through a temperature-controlled vessel containing twice-distilled water.

The outlet composition was recorded using an on line gas chromatograph (Shimadzu 14B), with pure He as carrier gas, equipped with a Thermal Conductivity Detector (TCD), set at T = 120 °C, and a Flame Ionization Detector (FID) for the detection of hydrocarbon compounds. Two chromatographic columns were employed for gas separation: a Porapack QS (1.83 m long and 0.0032 m diameter) for H_2 and CO and a Molecular Sieve 13X (3.05 m long and 0.0032 m diameter) for CO_2, CH_4 and light hydrocarbons, with both columns set at T = 80 °C. All gasification experiments were performed twice and the experimental error was less than 5%.

Results and discussion

Characterization of fuel samples

Biochar production

The production of biochars was carried out following the procedure described in Section Fuel feedstock preparation and biochars production. The solid fraction and condensed liquids were weighed in order to determine the corresponding yields of as-produced biochars, while the non-condensable gases were calculated by mass balance difference. The wt.% yield to solid (S), liquid (L) and gaseous (G) products during olive kernel thermal treatment at different temperatures is depicted in Fig. 2. By increasing the treatment temperature, the yield of the solid product (char) reduced from 59.8 wt% at 300 °C to 29.5 wt% and 25.9 wt% at 500 °C and 800 °C, respectively, while the yield to gaseous products was slightly increased from 26.8 wt% at 300 °C to 29.4 wt% at 500 °C and 33.8 wt% at 800 °C. The yield of liquids was maximized at the intermediate temperature of 500 °C (~41 wt%). In general, low treatment temperatures result mainly in solid products (char), while at higher temperatures gaseous products are favored via primary and secondary thermal cracking reactions [40].

Chemical analysis

The ultimate and proximate analyses of raw biomass and as-produced chars are illustrated in Table 1. As the pretreatment temperature increased to 800 °C, the carbon and fixed carbon contents increased from 50.2 to 86.5 wt% and from 13.9 to 79.7 wt%, respectively, whereas the H and O contents decreased from 5.9 to 0.8 wt% and 40.2 to 4.1 wt%, respectively. This indicates that slow pyrolysis at high temperatures enhances the carbonization degree of biochars through the decomposition of the organic matter in raw material. The content of volatile matter is substantially decreased with the increase of pyrolysis temperature, implying that the remaining organic content in biochars is gradually released upon

Please cite this article as: Lampropoulos A et al., Effect of Olive Kernel thermal treatment (torrefaction *vs.* slow pyrolysis) on the physicochemical characteristics and the CO_2 or H_2O gasification performance of as-prepared biochars, International Journal of Hydrogen Energy, https://doi.org/10.1016/j.ijhydene.2020.11.230

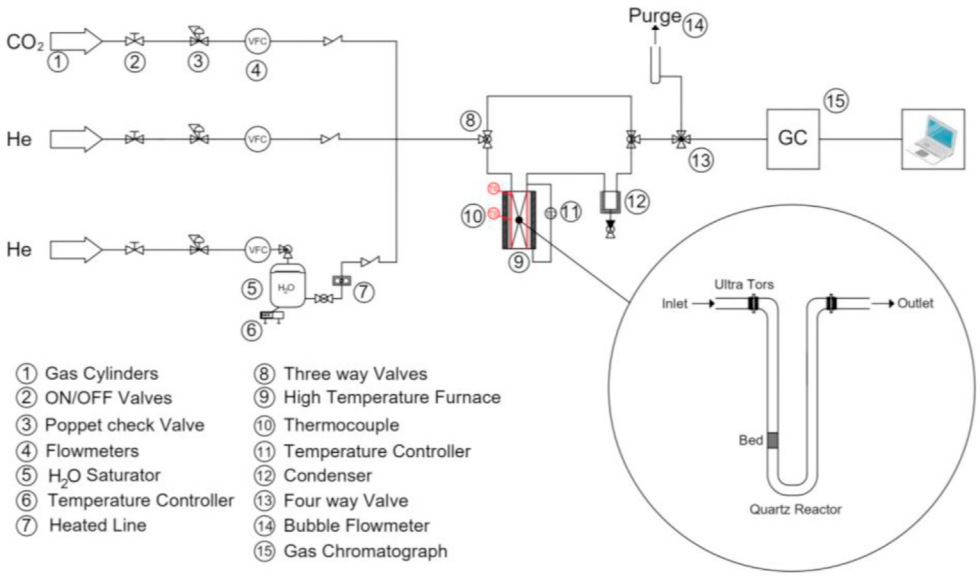

Fig. 1 – Schematic diagram of the experimental setup.

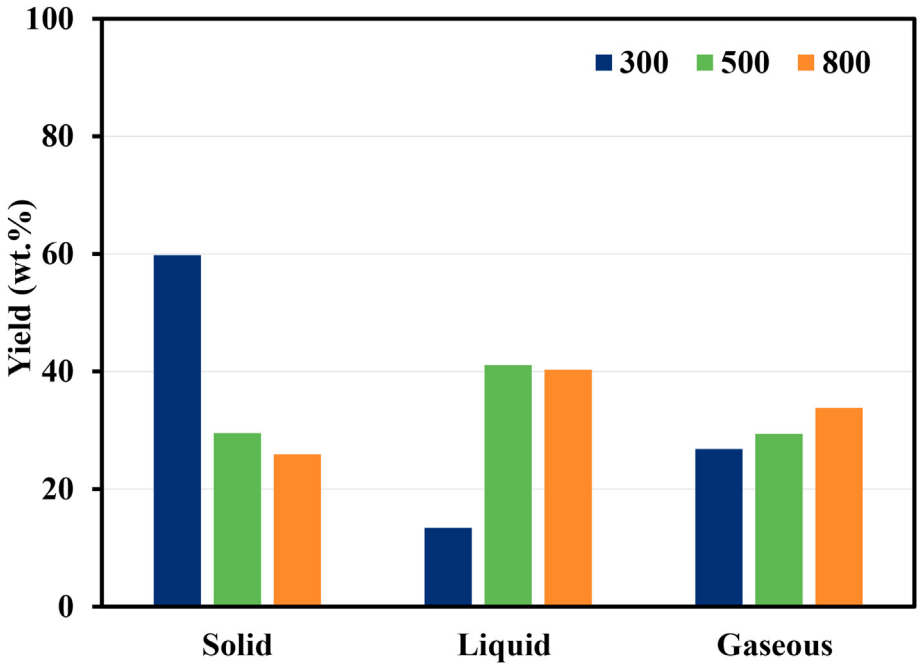

Fig. 2 – Solid, liquid and gas yields during olive kernel thermal treatment at 300, 500, and 800 °C, respectively.

Table 1 – Ultimate and proximate analyses and high heating values of the different fuel samples.

Samples	Ultimate analysis (wt.%)					Proximate analysis (wt.%)					Ratios		HHV[a]
	C	H	N	O	S	Moisture	Ash	Volatile matter	pH_{pzc}	Fixed carbon	H/C	O/C	
OK	50.2	5.9	0.7	40.2	0.02	7.4	2.9	75.8	–	13.9	1.41	0.60	20,020
OK300	63.4	5.2	1.0	26.5	0.10	4.0	3.9	54.3	8.2	37.8	0.98	0.31	25,497
OK500	81.9	2.9	0.8	8.0	nd[b]	4.5	6.4	15.0	10.8	74.1	0.42	0.07	30,037
OK800	86.5	0.8	0.8	4.1	0.10	6.4	7.8	6.1	12.2	79.7	0.11	0.04	31,116

[a] High Heating Value on a dry basis expressed in kJ/kg.
[b] Not detected.

Please cite this article as: Lampropoulos A et al., Effect of Olive Kernel thermal treatment (torrefaction *vs.* slow pyrolysis) on the physicochemical characteristics and the CO_2 or H_2O gasification performance of as-prepared biochars, International Journal of Hydrogen Energy, https://doi.org/10.1016/j.ijhydene.2020.11.230

thermal treatment [41]. It is worth mentioning that the olive kernel slowly pyrolyzed chars (OK500 and OK800) were mainly composed of fixed carbon with a content of 74.1 and 79.7 wt%, respectively.

Meanwhile the atomic ratio of H/C and O/C is gradually decreased from pristine OK to OK800 char, a trend which can be ascribed to the release of aromatic and other carbonaceous fragments upon thermal treatment of pristine OK [42,43]. Furthermore, the High Heating Value (HHV) substantially increases with heat treatment, which can be mainly attributed to the increase of carbon content [22]. Finally, an increase in the pH_{pzc} value at the point of zero charge of the as-produced biochars was observed upon increasing the treatment temperature, i.e., 8.2, 10.8 and 12.2 for OK300, OK500 and OK800 samples, respectively. The latter is ascribed to the increase of the ash content upon increasing the pyrolysis temperature, which is rich in alkali and alkaline earth metals (such as K, Ca, Na and Mg) giving rise to the basicity of fuel samples [42].

In Table 2, the wt.% content of the different main oxides contained in the ash of the pristine olive kernel and as-produced chars is depicted. All samples are mainly composed of K_2O, CaO and Na_2O, while substantially lower amounts of SO_3, P_2O_5, SiO_2, MgO, Fe_2O_3 and TiO_2 were also observed. Notably, the increase of pyrolysis temperature not only increased the ash content in the as-produced chars (Table 1) but also led to an increase in the concentration of MgO, CaO, Fe_2O_3 and K_2O. It has been reported [40,44] that the different counterparts of the ash might exhibit a different impact on the gasification performance, depending on their promoting or inhibiting role in the overall gasification reaction network. In general, alkali and alkaline earth metal oxides along with transition metal oxides, such as K_2O, Na_2O, CaO, MgO, and Fe_2O_3 exert a pronounced catalytic effect on the gasification performance [35–37]. Moreover, it is worth mentioning that Cl concentration follows a decreasing trend with increasing thermal treatment temperature, which is beneficial for the gasification process since chlorine could contribute to corrosion effects and toxic emissions [45].

Textural, morphological and structural analysis

The textural characteristics of all samples are depicted in Table 3. The helium density (d_{He}), representing the actual density of samples, practically remains the same for the raw (OK), torrefied (OK300) and mildly pyrolyzed (OK500) samples.

Table 2 – Main inorganic matter content (wt.%) relative to the total mass of ash, as revealed by the XRF analysis.

Oxide	OK	OK300	OK500	OK800
Na_2O	16.79	14.41	12.53	13.25
MgO	0.64	2.00	2.24	2.37
Al_2O_3	0.09	0.09	0.06	0.04
SiO_2	1.42	1.26	1.49	1.38
P_2O_5	3.88	4.46	4.30	4.35
Cl	7.27	6.52	3.26	3.71
SO_3	4.51	2.74	1.31	1.45
K_2O	46.91	52.48	57.92	53.61
CaO	17.58	14.84	16.36	18.46
Fe_2O_3	0.394	0.283	0.430	0.897
TiO_2	0.02	0.02	0.04	0.07

An obvious increase is observed upon increasing the treatment temperature to 800 °C (OK800), which could be attributed to the formation of a more condensed arrangement of the carbonaceous matter due to crosslinking and/or to the formation of packed planar clusters of aromatic rings [46]. In general, the removal of volatile matter upon thermal treatment results in the increase of porosity in the chars, as clearly shown in Table 3, leading to samples with an essentially macropore structure. As the temperature of thermal treatment increases, the porosity and pore volume (V_p) gradually increase. The low BET surface area (S_{BET}) observed in all fuel samples might be assigned to phenomena such as fusing, melting and carbonization that partially block micropores (i.e. pores <2 nm), which mainly contribute to BET surface area.

The SEM images of the pristine olive kernel and as-produced chars are shown in Figs. 3 and 4, respectively. SEM analysis of the pristine OK indicated particles with no specific morphology and high poly-dispersity with particle sizes ranging between 10 and 150 μm (Fig. 3). Even though the samples were sieved into fines of 100–200 μm, some smaller particles can be also detected, possibly due to their strong attachment to larger particles or their blockage in cavities. On the other hand, OK chars appeared in the form of truncated, irregular shapes and their pores are characterized by an open, oval structure and thick walling (Fig. 4).

All samples show a uniform distribution of the different counterparts as further verified by EDX analysis (Fig. 5). The inorganic matter consists mainly of K and Ca compounds, in consistency with XRF analysis (Table 2). Moreover, the carbon content is in a good agreement with ultimate and proximate analysis shown in Table 1.

The X-ray patterns of the investigated samples are shown in Fig. 6. Two bands are observed at 2θ ~23° and 44°, which correspond to the diffuse graphite (002) and (100) bands, respectively. In the XRD pattern of the raw OK sample, the sharp (002) band at 23° implies that the pristine biomass has a highly ordered structure. Moreover, raw biomass presented a band at about 15° (peak γ of aliphatic chain), ascribed to the radial spread of the aliphatic chains. Biochar samples illustrate broader bands, implying a more disordered structure, as further verified by Raman analysis (see below) [43,47].

Raman spectroscopy analysis

To further explore the crystallite structure, the Raman spectra of as-produced chars were acquired (Fig. 7). No distinct peaks could be observed in the case of raw OK sample and thus its respective spectrum is omitted from Fig. 7. The normalized intensity of the D-band (ca. 1350 cm^{-1}), is generally increased with both the number of amorphous carbon and disordered structure in graphite or other highly ordered carbonaceous materials. The G-band (ca. 1600 cm^{-1}), is attributed to the stretching vibration modes of graphite C=C bonds. The intensity of the G-band (I_G) is sharpened as the degree of graphitization increases [48]. Although, the position of the D and G peaks remain unchanged upon increasing the pyrolysis temperature [49], the I_D/I_G ratio is notably modified implying a different degree of carbon organization. In particular, the I_D/I_G ratio is 0.43, 0.59 and 0.82 for OK300, OK500 and OK800, respectively, denoting an increase of the share of disordered carbon and the breakdown in symmetry atoms with the

Please cite this article as: Lampropoulos A et al., Effect of Olive Kernel thermal treatment (torrefaction *vs.* slow pyrolysis) on the physicochemical characteristics and the CO_2 or H_2O gasification performance of as-prepared biochars, International Journal of Hydrogen Energy, https://doi.org/10.1016/j.ijhydene.2020.11.230

Table 3 – Textural characteristics of olive kernel and as-produced char samples.

Samples	d_{He} (g/cm^3)	Porosity (%)	V_p (cm^3/g)	V_{meso} (cm^3/g)	V_{macro} (cm^3/g)	S_{BET} (m^2/g)
OK	1.45	11	0.09	0.03	0.06	<3
OK300	1.35	14	0.14	0.04	0.10	<3
OK500	1.42	52	0.70	0.16	0.54	<3
OK800	1.81	56	1.00	0.00	1.00	<3

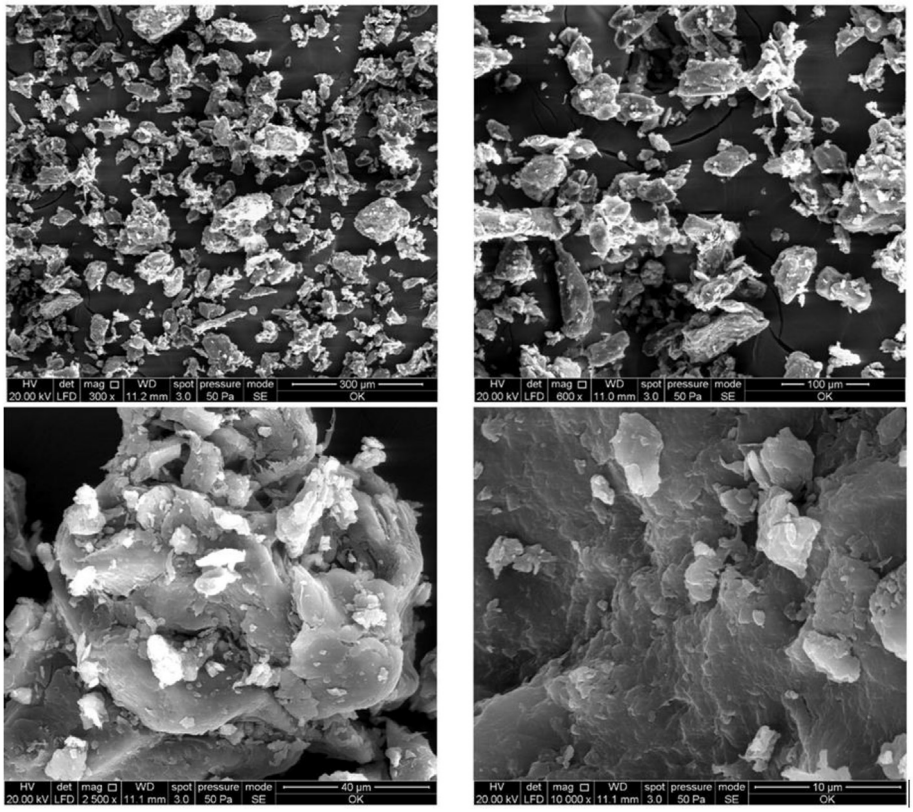

Fig. 3 – SEM micrographs of pristine olive kernel (OK) sample.

increase of the pretreatment temperature [50]. This behavior is also confirmed by the ratio of intensities of V and G bands, with the V band located in the valley between the D and G peaks, as depicted in Fig. 7. In general, the I_V/I_G ratio is increased with the decrease in the uniformity of carbonaceous structure [51]. In the present study, the I_V/I_G ratio equals to 0.25, 0.38 and 0.47 for OK300, OK500 and OK800, respectively, implying that the graphitization degree of fuel samples decreases as the pyrolysis temperature increase [52]. In view of this fact, it has been reported that higher I_D/I_G and I_V/I_G ratios could improve the gasification performance [48–51,53].

FTIR spectroscopy analysis

Fig. 8 shows the FTIR spectra of all samples. The band at ca. 3400 cm^{-1} is ascribed to O–H stretching vibration mode of hydroxyl functional groups. This band remained almost unchanged in all samples in agreement with the similar moisture content estimated in proximate analysis (Table 1). The strength of peak at ca. 2800 cm^{-1} corresponds to symmetric stretching vibration C–H bonds (mainly including the CH_2 and CH_3). The negligible intensity of this peak in the thermally treated samples aligns with the decreased volatile matter content. The band at 1730 cm^{-1}, which is attributed to C=O vibrations in carbonyl groups, is indicative of the presence of acetyl derived groups, aldehyde groups, etc. The absorbance peak between 1650 and 1450 cm^{-1} is assigned to the stretching vibration of aromatic rings C=C [28,42]. Hence, as the pyrolysis temperature increases, the absorbance peaks from all chemical functional groups become weaker.

In specific, in the case of pristine OK and OK300 char, the characteristic bands of hydroxyl, carboxyl, carbonyl and methoxyl functional groups are still clearly observed. On the contrary, the corresponding peaks for OK500 and OK800 samples are disappearing under thermal cracking. This observation is in line with the gradual decrease of the O/C and H/C ratios and the appearance of disordered carbonaceous

Please cite this article as: Lampropoulos A et al., Effect of Olive Kernel thermal treatment (torrefaction *vs.* slow pyrolysis) on the physicochemical characteristics and the CO_2 or H_2O gasification performance of as-prepared biochars, International Journal of Hydrogen Energy, https://doi.org/10.1016/j.ijhydene.2020.11.230

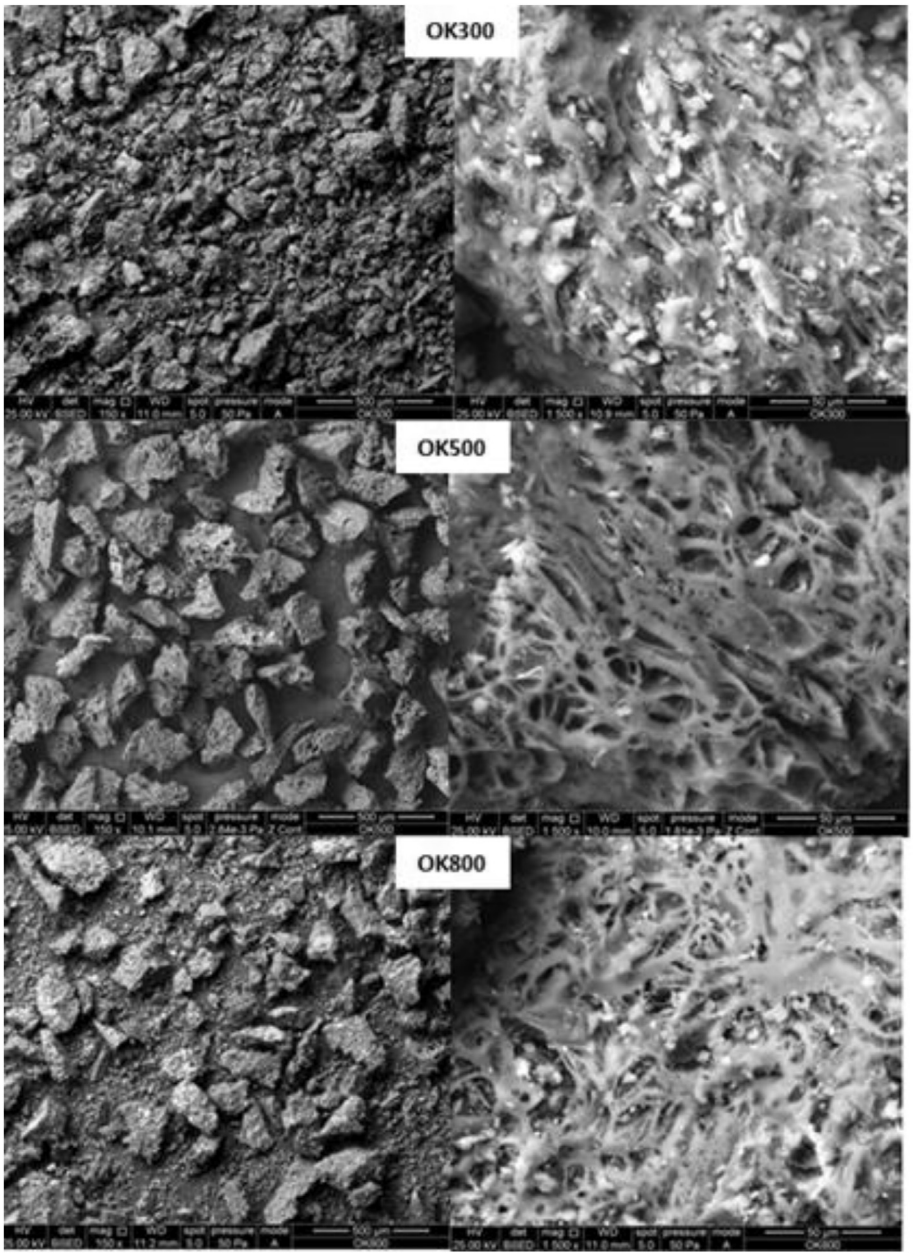

Fig. 4 – SEM micrographs of as-produced biochar samples.

structure upon thermal treatment, as revealed in Table 1 and Fig. 6, respectively.

Thermogravimetric analysis

A thermogravimetric analysis was carried out in the temperature range of 25–1000 °C under both inert (N_2) and reactive (CO_2) atmospheres, in order to gain insight into the reactivity of feedstock fuels (Fig. 9). Table 4 summarizes the total weight loss (wt.%) calculated for the different samples and atmospheres.

All samples present a similar weight loss profile under both N_2 and CO_2 flow up to a specific temperature (ca. 700–800 °C), where the samples start to interact with CO_2 via the reverse Boudouard reaction (Fig. 9). At low temperatures (ca. 100–120 °C) the mass loss detected is attributed to the removal of contained humidity. At the temperature range of 200–650 °C, there are two steps of weight loss attributed to primary (ca. 200–400 °C) and secondary (400–650 °C) devolatilization processes, which are clearly depicted for the pristine OK and OK300 char samples and are leveled off for the OK500 and OK800 chars, where the volatile matter content is low (Table 1). According to literature, primary devolatilization is attributed to the decomposition of hemi-cellulose and cellulose contained in lignocellulosic biomass samples mostly into light organic compounds, while the secondary devolatilization step is assigned to lignin content degradation [54,55]. Lignin is comprised of numerous aromatic sub-structures of carbon, which are slowly decomposed during pyrolysis, leaving condensed aromatic groups, as also revealed by the FTIR spectroscopy measurements (Fig. 8). The weight loss under

Please cite this article as: Lampropoulos A et al., Effect of Olive Kernel thermal treatment (torrefaction *vs.* slow pyrolysis) on the physicochemical characteristics and the CO_2 or H_2O gasification performance of as-prepared biochars, International Journal of Hydrogen Energy, https://doi.org/10.1016/j.ijhydene.2020.11.230

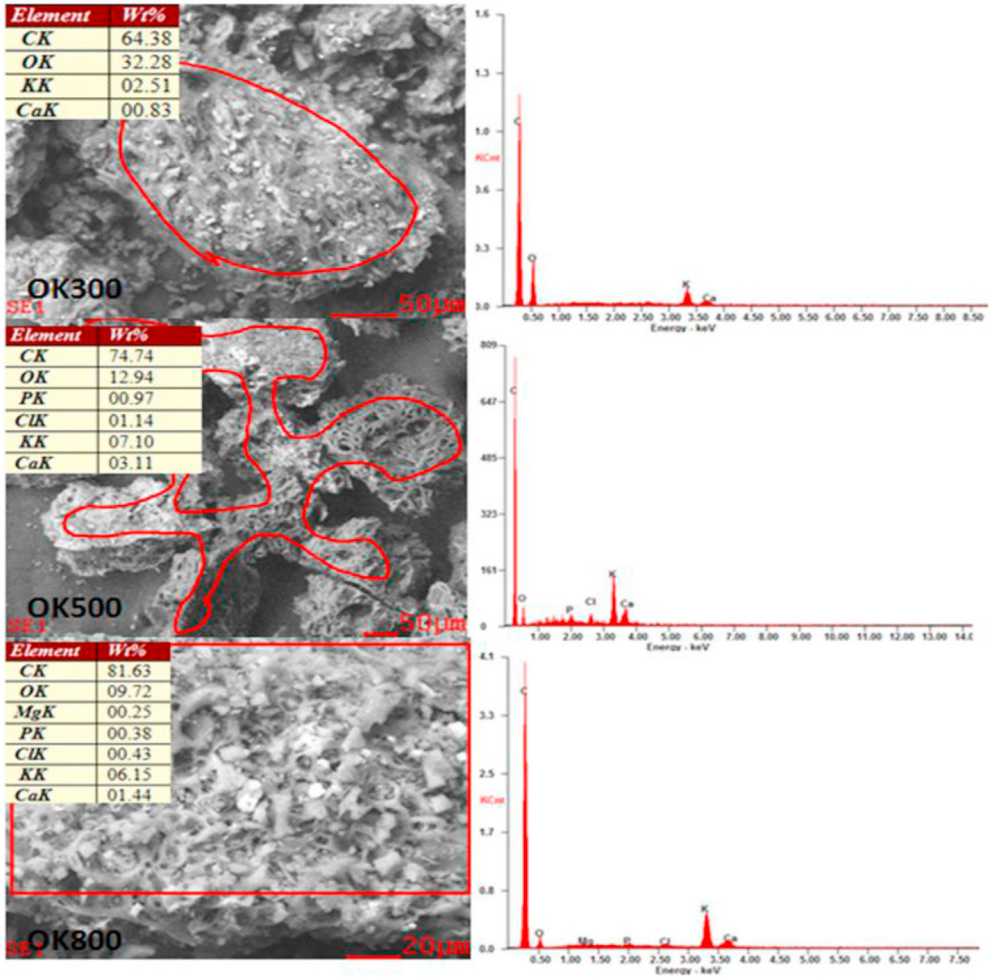

Fig. 5 – EDX analysis of the as-produced biochar samples.

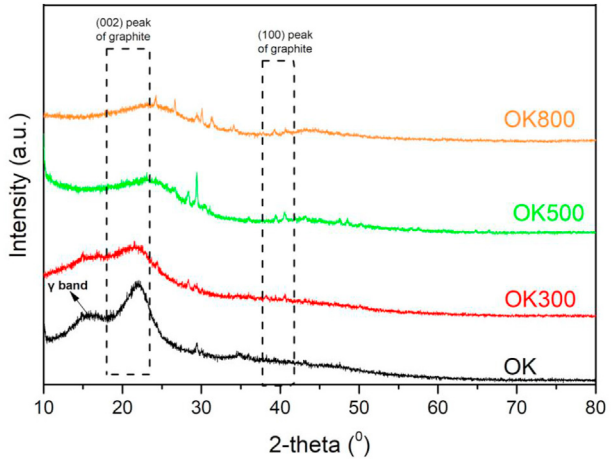

Fig. 6 – X-ray diffraction patterns of fuel samples.

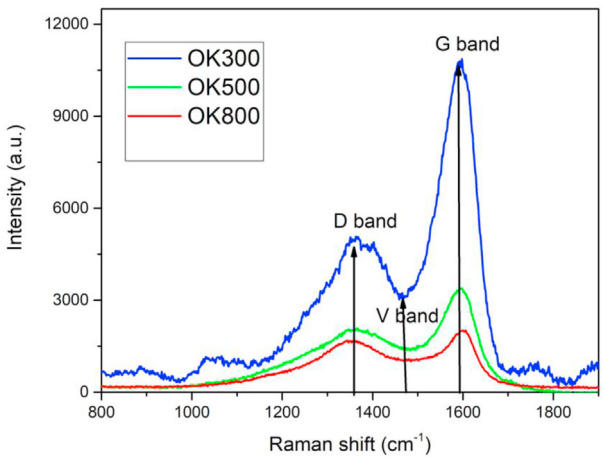

Fig. 7 – Raman spectra of thermally treated OK samples.

inert atmosphere is in accordance with the volatile matter content in the samples (Table 1), following the order: OK > OK300 > OK500 > OK800. Under CO_2 flow the additional weight loss at temperatures higher than 700 °C can be ascribed to the reaction of the remaining carbonaceous matter with CO_2 at elevated temperatures, where the reverse Boudouard reaction is thermodynamically favored [16], following the order: OK800 ≈ OK500 > OK300 > OK, in complete agreement with the fixed carbon content of fuel samples (Table 1). The residual weight of all samples at 1000 °C can be practically

Please cite this article as: Lampropoulos A et al., Effect of Olive Kernel thermal treatment (torrefaction *vs.* slow pyrolysis) on the physicochemical characteristics and the CO_2 or H_2O gasification performance of as-prepared biochars, International Journal of Hydrogen Energy, https://doi.org/10.1016/j.ijhydene.2020.11.230

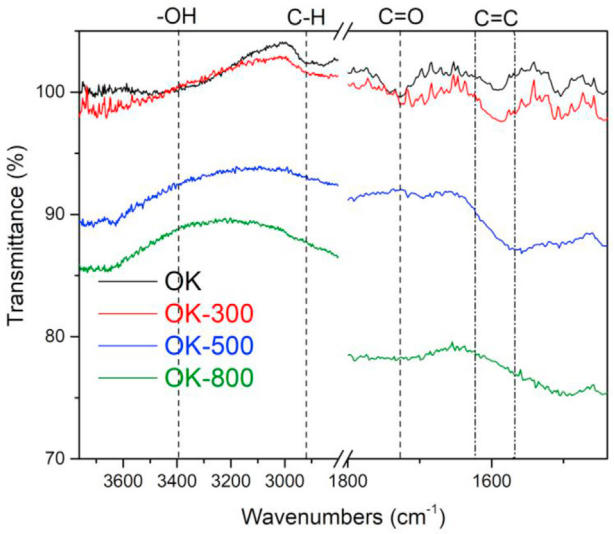

Fig. 8 – FTIR spectra of raw, torrefied and pyrolyzed OK samples.

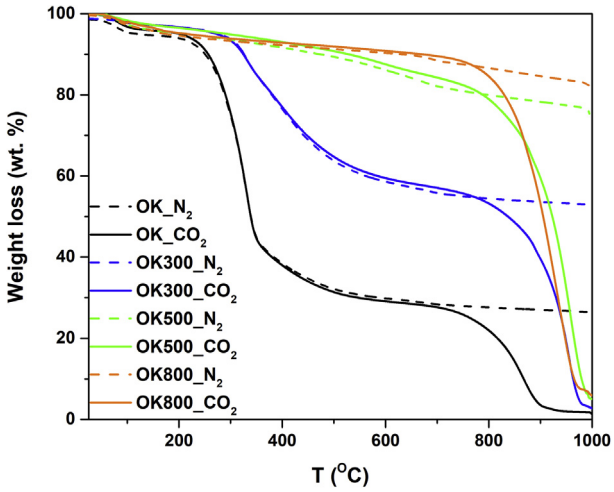

Fig. 9 – TGA profiles of the pristine and thermally treated OK samples under inert (N_2) and reactive (CO_2) atmospheres.

attributed to the amount of stable and unreactive ash, being in agreement with the proximate analysis (Table 1).

CO_2 and H_2O gasification performance

The gasification of biomass proceeds in two steps: the first step (at 200–650 °C) includes the evolution and decomposition of volatile matter and tar, and the second step involves the gasification of char at 650–1000 °C [56]. For the sake of results interpretation, the main reactions (R) taking place during biomass gasification are summarized below [5,57,58]:

Pyrolysis: $C_xH_yO_z \rightarrow$ Tar + CO_2 + CO + H_2 +CH_4 + H_2O (R1)

Tar cracking: Tar $\rightarrow$ CO_2 + CO + H_2 +CH_4 + light HCs (R2)

Tar dry cracking reaction: Tar + CO_2 $\rightarrow$ CO + H_2 +CH_4 + light HCs (R3)

Tar steam cracking reaction: Tar + n_1H_2O $\rightarrow$ n_2CO_2 + n_3H_2(R4)

Carbon/Char partial oxidation: C + ½ O_2 $\rightarrow$ CO, $\Delta H = -111$ kJ/mol (R5)

Carbon/Char oxidation: C + O_2 $\rightarrow$ CO_2, $\Delta H = -393$ kJ/mol (R6)

CO oxidation: CO + ½ O_2 $\rightarrow$ CO_2, $\Delta H = -283$ kJ/mol (R7)

H_2 oxidation: H_2 + ½ O_2 $\rightarrow$ H_2O, $\Delta H = -242$ kJ/mol (R8)

Water Gas Shift: CO + H_2O $\leftrightarrow$ CO_2 + H_2, $\Delta H = -41$ kJ/mol (R9)

Methanation: C + 2H_2 $\rightarrow$ CH_4, $\Delta H = -75$ kJ/mol (R10)

Reverse Boudouard: C + CO_2 $\rightarrow$ 2CO, $\Delta H = +172$ kJ/mol (R11)

Primary Steam Gasification: C + H_2O $\rightarrow$ CO + H_2, $\Delta H = +131$ kJ/mol (R12)

Secondary H_2O Gasification: C + 2H_2O $\rightarrow$ CO_2 + 2H_2, $\Delta H = +90$ kJ/mol (R13)

Steam Methane reforming: CH_4 + H_2O $\rightarrow$ CO + 3H_2, $\Delta H = +206$ kJ/mol (R14)

Fig. 10 depicts the effluent concentration (vol%) of CO_2 (a), CO (b), H_2 (c) and CH_4 (d) as a function of temperature, during the CO_2 gasification of olive kernel and as-produced chars.

The maximum consumption of CO_2 is obtained at ca. 750 °C (Fig. 10a), in consistency with the TGA results (Fig. 9), where the gasification reactions are thermodynamically favored [19,20]. Carbon monoxide, CO, was the primary product (Fig. 10b), starting to appear at ca. 600 °C, following an opposite trend to CO_2 consumption profile. The increase of CO concentration with temperature has been well documented in literature during the CO_2-aided gasification of various types of biomass [59–65]. Apart from CO, minor quantities of H_2 (Fig. 11c) and CH_4 (Fig. 11d) were also observed at lower temperatures, associated to the decomposition of released volatiles and homogeneous gas-phase reactions. This is in accordance with the onset temperature of reactions (R1), (R2), (R3) and (R4) [60,63,66].

Moreover, it is known that CO_2 reacts with tars, enhancing their cracking into hydrogen and light gaseous hydrocarbons [67–70]. Concerning hydrogen production, the first peak can be attributed to the pyrolysis step during gasification, while

Table 4 – Total weight loss (wt.%) of different feedstock fuels in TGA experiments.

TGA atmosphere	Weight loss (wt.%)			
	OK	OK300	OK500	OK800
N_2	72.5	46.1	25.6	18.2
CO_2	98.6	97.3	95.0	94.0

Please cite this article as: Lampropoulos A et al., Effect of Olive Kernel thermal treatment (torrefaction *vs.* slow pyrolysis) on the physicochemical characteristics and the CO_2 or H_2O gasification performance of as-prepared biochars, International Journal of Hydrogen Energy, https://doi.org/10.1016/j.ijhydene.2020.11.230

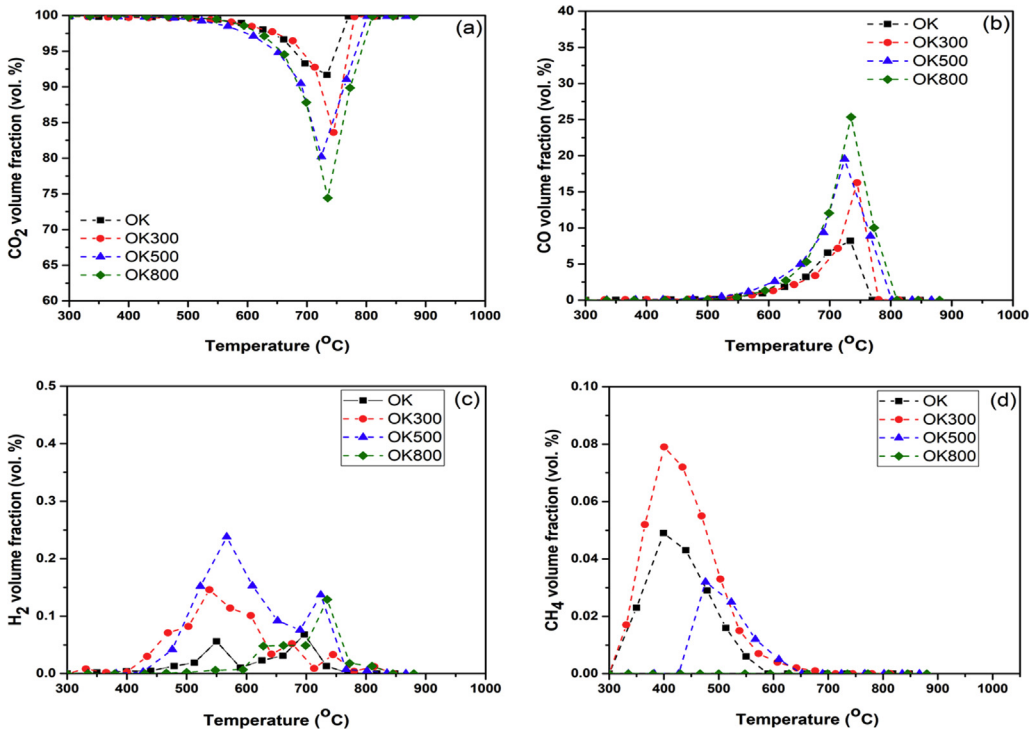

Fig. 10 – Volume fractions (vol%) of CO_2 (a), CO (b), H_2 (c) and CH_4 (d) during CO_2 gasification of olive kernel and as-produced chars. Reaction conditions: Fuel loading: 100 mg, agent: 100 vol% CO_2, flowrate: 30 cm^3/min.

the second peak is related to gas-phase reactions, such as the endothermic (R12), (R13) and (R14) reactions [67]. The negligible amounts of methane and hydrogen observed in the case of OK800 sample is in line with its limited content in volatile matter.

The corresponding results upon the employment of 10 vol % H_2O/He mixture as the gasification agent, are shown in Fig. 11. In this particular case, the gasification of biomass fuels is taking place at higher temperatures as compared to pure CO_2. In specific, the gasification reaction for the OK, OK300 and OK500 samples is terminated at 750, 850 and 900 °C, respectively, while OK800 runs out at 950 °C. The produced gas mixture consists mainly of H_2 and CO, followed by CO_2 and minor quantities of CH_4. The onset temperature for hydrogen production was ca. 500 °C for all samples. At higher temperatures the endothermic reactions R12, R13 and R14 are strongly favored and thus the formation of H_2 increases [17]. This is in agreement with several studies on biomass gasification, employing different feedstock such as legume straw, pine sawdust and pine bark [71–74]. Moreover, secondary cracking and reforming reactions of heavy hydrocarbons/tars can also contribute to hydrogen production at lower temperatures (up to 600 °C) [75].

Carbon monoxide, CO, concentration increases with temperature due both to R11 and R12 reactions [76]. High amounts of CO_2 are generated at low temperatures due to the oxidation (R6 and R7) and water gas shift (R9) reactions, which are highly exothermic. However, upon increasing the temperature, the CO_2 content in the effluent gas mixture starts to decrease at the expense of endothermic reactions prevailing in the high temperature region, such as the reverse Boudouard (R11) and reverse Water Gas Shift (R9) reactions [77,78]. Noticeably, both CO_2 and CO exhibit a significant production at 300 °C. According to Butterman and Castaldi [21], thermal cracking reactions at low temperatures result in the decomposition of biomass lattice, leading to oxygen release by the oxygenated functional groups and minerals, followed by char oxidation toward CO and CO_2 (R5 and R6 reactions).

Regarding CH_4 production, a double peak at the same temperature range is observed mostly in the case of OK, OK300 and OK500 samples. The first peak at lower temperatures (ca. 300–500 °C) is attributed to the pyrolysis and tar thermal cracking processes, while the second peak (above 500 °C) is ascribed to the gas phase methanation reactions (such as R10) [22]. The thermally treated sample at 800 °C exhibits only the second peak (above 500 °C), confirming the downward trend of the volatile matter content with the increase of the pretreatment temperature (Table 1).

The total amount (mmol/g) of generated CO_2, CO, H_2 and CH_4 during the aforementioned gasification processes was calculated from the integrated area of the respective curves in Figs. 10 and 11, and the results are summarized in Table 5.

As mentioned above, during CO_2 gasification, CO was the main product. Torrefaction at 300 °C exerts a moderate impact on CO yield, resulting in an increase of CO amount from 51.3 mmol/g (OK) to 70.3 mmol/g (OK300). However, slow

Please cite this article as: Lampropoulos A et al., Effect of Olive Kernel thermal treatment (torrefaction *vs.* slow pyrolysis) on the physicochemical characteristics and the CO_2 or H_2O gasification performance of as-prepared biochars, International Journal of Hydrogen Energy, https://doi.org/10.1016/j.ijhydene.2020.11.230

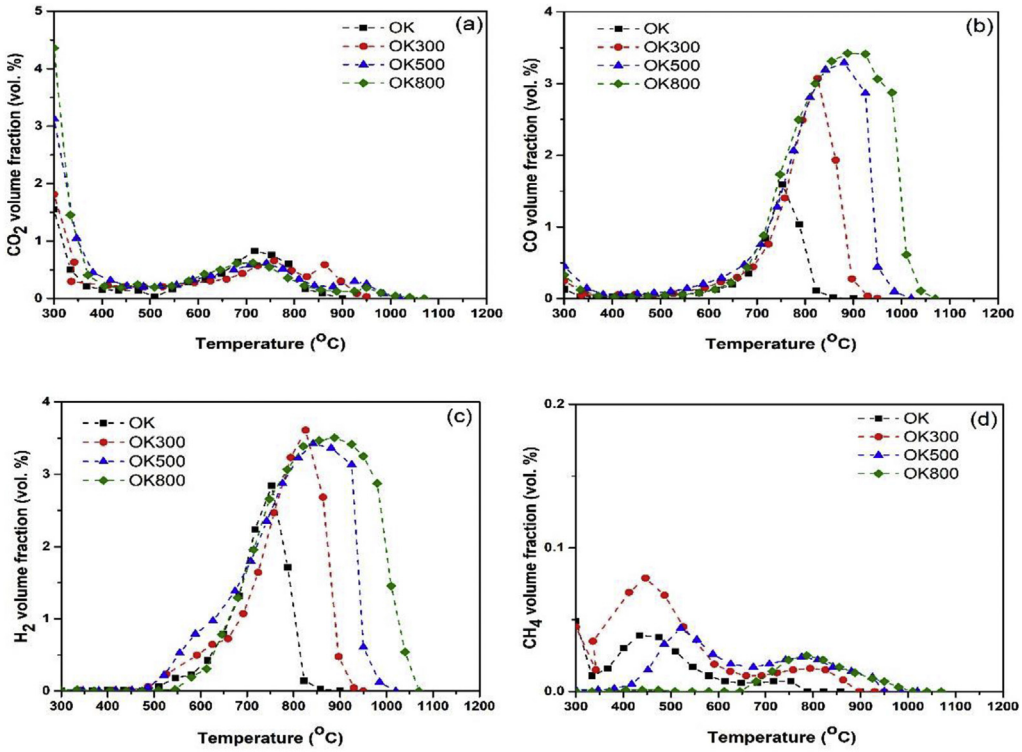

Fig. 11 – Volume fractions (vol%) of CO_2 (a), CO (b), H_2 (c) and CH_4 (d) during steam gasification of olive kernel and as-produced chars. Reaction conditions: Fuel loading: 100 mg, agent: 10 vol% H_2O/He, flowrate: 30 cm^3/min.

pyrolysis at 500 °C (OK500) results in a notable increase of CO amount (123.6 mmol/g), which, however, is not significantly altered (137 mmol/g) upon further increasing the pyrolysis temperature to 800 °C. The corresponding methane and hydrogen production were two orders of magnitude lower than the respective CO values and remained almost unaffected regardless of the pretreatment conditions.

When H_2O was employed as gasifying agent, the amount of the main constituents of the produced gas mixture (H_2, CO, CO_2) is increased, as in the case of CO_2 gasification experiments (Table 5), following the order of OK800 > OK500 > OK300 > OK. Regarding the H_2/CO molar ratio (Table 5), it varies between 1.2 and 2.3, implying its suitability not only for Fisher-Tropsh synthesis and methanol production but also for oxo-synthesis processes [13,14,37].

Table 5 – Production of gaseous products during CO_2 and H_2O gasification.

	CO_2 Gasification				
	CO production (mmol/g)	H_2 production (mmol/g)	CH_4 production (mmol/g)		
OK	51.3	0.7	0.4		
OK300	70.3	1.3	0.7		
OK500	123.6	2.4	0.2		
OK800	137.0	0.8	0.0		
	H_2O Gasification				
	CO_2 production (mmol/g)	CO production (mmol/g)	H_2 production (mmol/g)	CH_4 production (mmol/g)	H_2/CO
OK	12.8	9.0	20.8	0.5	2.3
OK300	14.8	24.1	36.3	1.1	1.5
OK500	20.0	44.0	58.3	0.7	1.3
OK800	20.0	55.0	62.7	0.3	1.2

On the basis of the present findings, it could be argued that the thermal pretreatment of pristine biomass (OK) notably modifies the solid state properties of as-produced chars with great implications on the gasification performance. In particular, the increase of pretreatment temperature leads to chars with: i) improved textural properties (higher porosity), ii) less ordered structure and higher fixed carbon content, iii) lower volatile matter content, iv) higher content in ash elements that could act as gasification catalysts (e.g. CaO, MgO, K_2O, Na_2O, and Fe_2O_3), and v) lower H/C and O/C ratios. Interestingly, the fixed carbon content, ash content, porosity as well as the I_D/I_G ratio follow in general the same trend as the syngas production, regardless of the gasification agent used (CO_2 or H_2O), i.e., OK800 > OK500 > OK300 > OK, implying their vital role in gasification performance. The opposite trend is observed for the volatile matter and the H/C and O/C atomic ratios. The latter is clearly demonstrated in Fig. 12a and b, where the impact of the above mentioned parameters on the syngas production (determined as the total amount of produced CO_x, H_2, CH_4 - Table 5) under both carbon dioxide and steam gasification conditions is depicted.

The beneficial effect of the above mentioned parameters is in accordance to the literature [22,27,43,47,75,79–81]. For instance, Wang et al. [79] studied the impact of pyrolysis

Please cite this article as: Lampropoulos A et al., Effect of Olive Kernel thermal treatment (torrefaction *vs.* slow pyrolysis) on the physicochemical characteristics and the CO_2 or H_2O gasification performance of as-prepared biochars, International Journal of Hydrogen Energy, https://doi.org/10.1016/j.ijhydene.2020.11.230

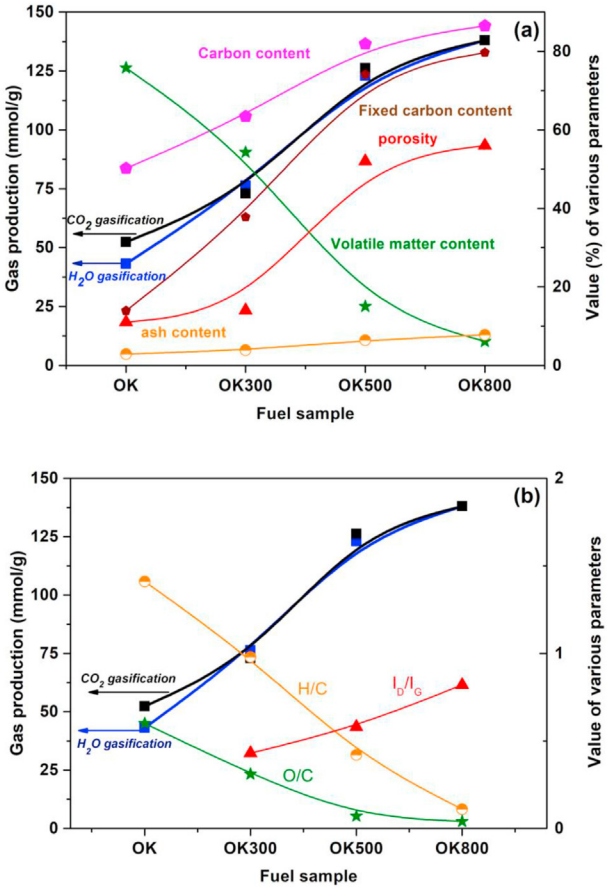

Fig. 12 – Relationship of the total amount of produced gas under CO_2 and H_2O gasification and the physicochemical characteristics of fuel samples (a, b).

temperature on the properties of woody biomass, focusing on the gasification reactivity under CO_2 atmosphere. They found that biocarbon produced at 800 °C had higher reactivity compared to that produced at 650 °C, due to its lower content on volatiles and higher fixed carbon content. Franco et al. [82] and Duman et al. [27], highlighted the role of metal oxides included in the ash as catalysts for the primary and secondary reactions taking place during the gasification process. The increase in indigenous mineral matters in char led to a markedly increased gasification reactivity as compared with that of the raw one. In a similar manner, Guo et al. [51] revealed the beneficial role of alkali and alkaline earth metals in the gasification performance of chars derived from wood, grape marc and macroalgae. Moreover, the I_D/I_G ratio is a crucial factor to evaluate gasification reactivity of biomass chars. In general, carbonaceous matter with high I_D/I_G ratio becomes more reactive and results in higher gasification performance [48–51,53].

Conclusion

The impact of pyrolytic pretreatment temperature (300, 500, 800 °C) on the physicochemical properties and the gasification performance of biochars derived from Greek olive kernel biomass, was investigated in the present work. The results clearly revealed that regardless the gasification agent (CO_2 or H_2O) used, an increase on the amount of gaseous products (mainly CO, CO_2, H_2 and CH_4) is observed upon increasing the pretreatment temperature, following the order: OK800 > OK500 > OK300 > OK. The observed trend in gasification performance is closely correlated with the increase in carbon and fixed carbon content, ash content and I_D/I_G ratio and the corresponding decrease of H/C and O/C ratios and volatile matter content, upon the increase of pretreatment temperature. Moreover, the gasification agent employed notably affects the composition of the generated bio-syngas. In the case of CO_2 gasification, the main gas produced is CO with negligible amounts of H_2 and CH_4. On the other hand, steam gasification leads to a mixture rich in H_2, CO and CO_2 with a H_2/CO ratio varying between 1.2 and 2.3. Although the optimum gasification performance in terms of gas production were obtained for the OK500 and OK800 chars, further techno-economic analysis, taking into consideration the solid yields and energy requirements during the char production, is required to assess the overall gasification process and to conclude about the best fuel feedstock. Work is in progress towards this direction.

Author contribution

M.A.M.M., A.A., A.M., V.B. and C.A. contributed to samples preparation and characterization; A.L and N.K. contributed to gasification studies; M.K. and G.E.M. contributed to the conception, design and results interpretation; M.K. and G.E.M. validated the results and administered the project. A.L. wrote the original draft. Finally, G.E.M. reviewed, edited and submitted the manuscript in the final form. All authors contributed to the discussion, read and approved the final version of the manuscript.

Declaration of competing interest

The authors declare that they have no known competing financial interests or personal relationships that could have appeared to influence the work reported in this paper.

Acknowledgements

This research has been co-financed by the European Union and Greek national funds through the Operational Program Competitiveness, Entrepreneurship and Innovation, under the call RESEARCH - CREATE - INNOVATE (project code: T1EDK-01894).

REFERENCES

[1] Mulvaney D. Green new deal. Sol Power 2019:47–65. https://doi.org/10.2307/j.ctvd1c6zh.7.

[2] Schöpe M. Renewable energy directive. In: Eur wind energy conf exhib 2008, vol. 1; 2008. p. 32–8.
[3] Scarlat N, Fahl F, Lugato E, Monforti-Ferrario F, Dallemand JF. Integrated and spatially explicit assessment of sustainable crop residues potential in Europe. Biomass Bioenergy 2019;122:257–69. https://doi.org/10.1016/j.biombioe.2019.01.021.
[4] Alatzas S, Moustakas K, Malamis D, Vakalis S. Biomass potential from agricultural waste for energetic utilization in Greece. Energies 2019;12. https://doi.org/10.3390/en12061095.
[5] Farzad S, Mandegari MA, Görgens JF. A critical review on biomass gasification, co-gasification, and their environmental assessments. Biofuel Res J 2016;3:483–95. https://doi.org/10.18331/BRJ2016.3.4.3.
[6] Sahu SG, Chakraborty N, Sarkar P. Coal-biomass co-combustion: an overview. Renew Sustain Energy Rev 2014;39:575–86. https://doi.org/10.1016/j.rser.2014.07.106.
[7] Kan T, Strezov V, Evans TJ. Lignocellulosic biomass pyrolysis: a review of product properties and effects of pyrolysis parameters. Renew Sustain Energy Rev 2016;57:1126–40. https://doi.org/10.1016/j.rser.2015.12.185.
[8] Wu H, Xiao J, Zeng X, Li X, Yang J, Zou Y, et al. A high performance direct carbon solid oxide fuel cell – a green pathway for brown coal utilization. Appl Energy 2019;248:679–87. https://doi.org/10.1016/j.apenergy.2019.04.104.
[9] Elleuch A, Halouani K, Li Y. Investigation of chemical and electrochemical reactions mechanisms in a direct carbon fuel cell using olive wood charcoal as sustainable fuel. J Power Sources 2015;281:350–61. https://doi.org/10.1016/j.jpowsour.2015.01.171.
[10] Jafri N, Wong WY, Doshi V, Yoon LW, Cheah KH. A review on production and characterization of biochars for application in direct carbon fuel cells. Process Saf Environ Protect 2018;118:152–66. https://doi.org/10.1016/j.psep.2018.06.036.
[11] Corigliano O, Fragiacomo P. Extensive analysis of SOFC fed by direct syngas at different anodic compositions by using two numerical approaches. Energy Convers Manag 2020;209:112664. https://doi.org/10.1016/j.enconman.2020.112664.
[12] Athanasiou C, Coutelieris F, Vakouftsi E, Skoulou V, Antonakou E, Marnellos G, et al. From biomass to electricity through integrated gasification/SOFC system-optimization and energy balance. Int J Hydrogen Energy 2007;32:337–42. https://doi.org/10.1016/j.ijhydene.2006.06.048.
[13] Ren J, Liu YL, Zhao XY, Cao JP. Methanation of syngas from biomass gasification: an overview. Int J Hydrogen Energy 2020;45:4223–43. https://doi.org/10.1016/j.ijhydene.2019.12.023.
[14] 2016 Synthetic natural gas: from coal, dry biomass, and power-to-gas applications. 2016. https://doi.org/10.1016/j.focat.2016.07.047.
[15] Santos RG dos, Alencar AC. Biomass-derived syngas production via gasification process and its catalytic conversion into fuels by Fischer Tropsch synthesis: a review. Int J Hydrogen Energy 2020;45:18114–32. https://doi.org/10.1016/j.ijhydene.2019.07.133.
[16] Ren J, Cao JP, Zhao XY, Yang FL, Wei XY. Recent advances in syngas production from biomass catalytic gasification: a critical review on reactors, catalysts, catalytic mechanisms and mathematical models. Renew Sustain Energy Rev 2019;116:109426. https://doi.org/10.1016/j.rser.2019.109426.
[17] Parthasarathy P, Narayanan KS. Hydrogen production from steam gasification of biomass: influence of process parameters on hydrogen yield - a review. Renew Energy 2014;66:570–9. https://doi.org/10.1016/j.renene.2013.12.025.
[18] Thomson R, Kwong P, Ahmad E, Nigam KDP. Clean syngas from small commercial biomass gasifiers; a review of gasifier development, recent advances and performance evaluation. Int J Hydrogen Energy 2020;45:21087–111. https://doi.org/10.1016/j.ijhydene.2020.05.160.
[19] Lahijani P, Zainal ZA, Mohammadi M, Mohamed AR. Conversion of the greenhouse gas CO_2 to the fuel gas CO via the Boudouard reaction: a review. Renew Sustain Energy Rev 2015;41:615–32. https://doi.org/10.1016/j.rser.2014.08.034.
[20] Renganathan T, Yadav MV, Pushpavanam S, Voolapalli RK, Cho YS. CO_2 utilization for gasification of carbonaceous feedstocks: a thermodynamic analysis. Chem Eng Sci 2012;83:159–70. https://doi.org/10.1016/j.ces.2012.04.024.
[21] Butterman HC, Castaldi MJ. CO_2 as a carbon neutral fuel source via enhanced biomass gasification. Environ Sci Technol 2009;43:9030–7. https://doi.org/10.1021/es901509n.
[22] Tripathi M, Sahu JN, Ganesan P. Effect of process parameters on production of biochar from biomass waste through pyrolysis: a review. Renew Sustain Energy Rev 2016;55:467–81. https://doi.org/10.1016/j.rser.2015.10.122.
[23] Cetin E, Moghtaderi B, Gupta R, Wall TF. Influence of pyrolysis conditions on the structure and gasification reactivity of biomass chars. Fuel 2004;83:2139–50. https://doi.org/10.1016/j.fuel.2004.05.008.
[24] Asadullah M, Zhang S, Min Z, Yimsiri P, Li CZ. Effects of biomass char structure on its gasification reactivity. Bioresour Technol 2010;101:7935–43. https://doi.org/10.1016/j.biortech.2010.05.048.
[25] Okumura Y, Hanaoka T, Sakanishi K. Effect of pyrolysis conditions on gasification reactivity of woody biomass-derived char. Proc Combust Inst 2009;32 II:2013–20. https://doi.org/10.1016/j.proci.2008.06.024.
[26] He Q, Guo Q, Ding L, Wei J, Yu G. CO_2 gasification of char from raw and torrefied biomass: reactivity, kinetics and mechanism analysis. Bioresour Technol 2019;293. https://doi.org/10.1016/j.biortech.2019.122087.
[27] Duman G, Uddin MA, Yanik J. The effect of char properties on gasification reactivity. Fuel Process Technol 2014;118:75–81. https://doi.org/10.1016/j.fuproc.2013.08.006.
[28] Min F, Zhang M, Zhang Y, Cao Y, Pan WP. An experimental investigation into the gasification reactivity and structure of agricultural waste chars. J Anal Appl Pyrolysis 2011;92:250–7. https://doi.org/10.1016/j.jaap.2011.06.005.
[29] Ren S, Lei H, Wang L, Bu Q, Chen S, Wu J, et al. The effects of torrefaction on compositions of bio-oil and syngas from biomass pyrolysis by microwave heating. Bioresour Technol 2013;135:659–64. https://doi.org/10.1016/j.biortech.2012.06.091.
[30] Bouraoui Z, Jeguirim M, Guizani C, Limousy L, Dupont C, Gadiou R. Thermogravimetric study on the influence of structural, textural and chemical properties of biomass chars on CO_2 gasification reactivity. Energy 2015;88:703–10. https://doi.org/10.1016/j.energy.2015.05.100.
[31] Jiang L, Hu S, Wang Y, Su S, Sun L, Xu B, et al. Catalytic effects of inherent alkali and alkaline earth metallic species on steam gasification of biomass. Int J Hydrogen Energy 2015;40:15460–9. https://doi.org/10.1016/j.ijhydene.2015.08.111.
[32] Huang Y, Yin X, Wu C, Wang C, Xie J, Zhou Z, et al. Effects of metal catalysts on CO_2 gasification reactivity of biomass char. Biotechnol Adv 2009;27:568–72. https://doi.org/10.1016/j.biotechadv.2009.04.013.

Please cite this article as: Lampropoulos A et al., Effect of Olive Kernel thermal treatment (torrefaction *vs.* slow pyrolysis) on the physicochemical characteristics and the CO_2 or H_2O gasification performance of as-prepared biochars, International Journal of Hydrogen Energy, https://doi.org/10.1016/j.ijhydene.2020.11.230

[33] Hognon C, Dupont C, Grateau M, Delrue F. Comparison of steam gasification reactivity of algal and lignocellulosic biomass: influence of inorganic elements. Bioresour Technol 2014;164:347–53. https://doi.org/10.1016/j.biortech.2014.04.111.
[34] International olive council. n.d, https://www.internationaloliveoil.org. https://www.internationaloliveoil.org.
[35] Zabaniotou A, Stavropoulos G, Skoulou V. Activated carbon from olive kernels in a two-stage process: industrial improvement. Bioresour Technol 2008;99:320–6. https://doi.org/10.1016/j.biortech.2006.12.020.
[36] Skoulou V, Zabaniotou A, Stavropoulos G, Sakelaropoulos G. Syngas production from olive tree cuttings and olive kernels in a downdraft fixed-bed gasifier. Int J Hydrogen Energy 2008;33:1185–94. https://doi.org/10.1016/j.ijhydene.2007.12.051.
[37] Skoulou V, Koufodimos G, Samaras Z, Zabaniotou A. Low temperature gasification of olive kernels in a 5-kW fluidized bed reactor for H_2-rich producer gas. Int J Hydrogen Energy 2008;33:6515–24. https://doi.org/10.1016/j.ijhydene.2008.07.074.
[38] García-Ibañez P, Cabanillas A, Sánchez JM. Gasification of leached orujillo (olive oil waste) in a pilot plant circulating fluidised bed reactor. Preliminary results. Biomass and Bioenergy 2004;27:183–94. https://doi.org/10.1016/j.biombioe.2003.11.007.
[39] Calvo EG, Rey-Raap N, Arenillas A, Menéndez JA. The effect of the carbon surface chemistry and electrolyte pH on the energy storage of supercapacitors. RSC Adv 2014;4:32398–404. https://doi.org/10.1039/c4ra04430d.
[40] Vamvuka D, Kakaras E, Kastanaki E, Grammelis P. Pyrolysis characteristics and kinetics of biomass residuals mixtures with lignite. Fuel 2003;82:1949–60. https://doi.org/10.1016/S0016-2361(03)00153-4.
[41] Diao R, Zhu X, Wang C, Zhu X. Synergistic effect of physicochemical properties and reaction temperature on gasification reactivity of walnut shell chars. Energy Convers Manag 2020;204:112313. https://doi.org/10.1016/j.enconman.2019.112313.
[42] Ma Z, Yang Y, Ma Q, Zhou H, Luo X, Liu X, et al. Evolution of the chemical composition, functional group, pore structure and crystallographic structure of bio-char from palm kernel shell pyrolysis under different temperatures. J Anal Appl Pyrolysis 2017;127:350–9. https://doi.org/10.1016/j.jaap.2017.07.015.
[43] Fu P, Yi W, Bai X, Li Z, Hu S, Xiang J. Effect of temperature on gas composition and char structural features of pyrolyzed agricultural residues. Bioresour Technol 2011;102:8211–9. https://doi.org/10.1016/j.biortech.2011.05.083.
[44] Kaklidis N, Strandbakke R, Arenillas A, Menéndez JA, Konsolakis M, Marnellos GE. The synergistic catalyst-carbonates effect on the direct bituminous coal fuel cell performance. Int J Hydrogen Energy 2019;44:10033–42. https://doi.org/10.1016/j.ijhydene.2019.02.038.
[45] Vamvuka D, Zografos D. Predicting the behaviour of ash from agricultural wastes during combustion. Fuel 2004;83:2051–7. https://doi.org/10.1016/j.fuel.2004.04.012.
[46] Prauchner MJ, Pasa VMD, Molhallem NDS, Otani C, Otani S, Pardini LC. Structural evolution of Eucalyptus tar pitch-based carbons during carbonization. Biomass Bioenergy 2005;28:53–61. https://doi.org/10.1016/j.biombioe.2004.05.004.
[47] Diao R, Zhu X, Wang C, Zhu X. Synergistic effect of physicochemical properties and reaction temperature on gasification reactivity of walnut shell chars. Energy Convers Manag 2020;204. https://doi.org/10.1016/j.enconman.2019.112313.
[48] Wang G, Zhang J, Shao J, Liu Z, Wang H, Li X, et al. Experimental and modeling studies on CO_2 gasification of biomass chars. Energy 2016;114:143–54. https://doi.org/10.1016/j.energy.2016.08.002.
[49] Bar-Ziv E, Zaida A, Salatino P, Senneca O. Diagnostics of carbon gasification by Raman microprobe spectroscopy. Proc Combust Inst 2000;28:2369–74. https://doi.org/10.1016/S0082-0784(00)80649-9.
[50] Tladanein K. Influence of inherent alkali content and surface area of biomass char on its CO_2 gasification reactivity. Iran J Energy Environ 2017;12:395–9. https://doi.org/10.5829/idosi.ijee.2017.08.01.01.
[51] Guo P, Saw WL, Van Eyk PJ, Stechel EB, De Nys R, Ashman PJ, et al. Gasification reactivity and physicochemical properties of the chars from raw and torrefied wood, grape marc, and macroalgae. Energy Fuels 2017;31:2246–59. https://doi.org/10.1021/acs.energyfuels.6b02215.
[52] Li R, Zhang J, Wang G, Ning X, Wang H, Wang P. Study on CO_2 gasification reactivity of biomass char derived from high-temperature rapid pyrolysis. Appl Therm Eng 2017;121:1022–31. https://doi.org/10.1016/j.applthermaleng.2017.04.132.
[53] Guizani C, Haddad K, Limousy L, Jeguirim M. New insights on the structural evolution of biomass char upon pyrolysis as revealed by the Raman spectroscopy and elemental analysis. Carbon N Y 2017;119:519–21. https://doi.org/10.1016/j.carbon.2017.04.078.
[54] Lee Y, Park J, Ryu C, Gang KS, Yang W, Park YK, et al. Comparison of biochar properties from biomass residues produced by slow pyrolysis at 500°C. Bioresour Technol 2013;148:196–201. https://doi.org/10.1016/j.biortech.2013.08.135.
[55] Acevedo-Páez JC, Durán JM, Posso F, Arenas E. Hydrogen production from palm kernel shell: kinetic modeling and simulation. Int J Hydrogen Energy 2020;45:25689–97. https://doi.org/10.1016/j.ijhydene.2019.10.146.
[56] Duman G, Uddin MA, Yanik J. Hydrogen production from algal biomass via steam gasification. Bioresour Technol 2014;166:24–30. https://doi.org/10.1016/j.biortech.2014.04.096.
[57] Sikarwar VS, Zhao M, Clough P, Yao J, Zhong X, Memon MZ, et al. An overview of advances in biomass gasification. Energy Environ Sci 2016;9:2939–77. https://doi.org/10.1039/c6ee00935b.
[58] Kirubakaran V, Sivaramakrishnan V, Nalini R, Sekar T, Premalatha M, Subramanian P. A review on gasification of biomass. Renew Sustain Energy Rev 2009;13:179–86. https://doi.org/10.1016/j.rser.2007.07.001.
[59] Ahmed I, Gupta AK. Characteristics of cardboard and paper gasification with CO_2. Appl Energy 2009;86:2626–34. https://doi.org/10.1016/j.apenergy.2009.04.002.
[60] Yao X, Yu Q, Xie H, Duan W, Han Z, Liu S, et al. Syngas production through biomass/CO_2 gasification using granulated blast furnace slag as heat carrier. J Renew Sustain Energy 2017;9. https://doi.org/10.1063/1.4993259.
[61] Sadhwani N, Adhikari S, Eden MR. Biomass gasification using carbon dioxide: effect of temperature, CO_2/C ratio, and the study of reactions influencing the process. Ind Eng Chem Res 2016;55:2883–91. https://doi.org/10.1021/acs.iecr.5b04000.
[62] Link S, Tran KQ, Bach QV, Yrjas P, Lindberg D, Arvelakis S, et al. Catalytic effect of oil shale ash on CO_2 gasification of leached wheat straw and reed chars. Energy 2018;152:906–13. https://doi.org/10.1016/j.energy.2018.04.013.
[63] Cheng Y, Thow Z, Wang CH. Biomass gasification with CO_2 in a fluidized bed. Powder Technol 2016;296:87–101. https://doi.org/10.1016/j.powtec.2014.12.041.
[64] Ratchahat S, Kodama S, Tanthapanichakoon W, Sekiguchi H. CO_2 gasification of biomass wastes enhanced by Ni/Al2O3

Please cite this article as: Lampropoulos A et al., Effect of Olive Kernel thermal treatment (torrefaction *vs.* slow pyrolysis) on the physicochemical characteristics and the CO_2 or H_2O gasification performance of as-prepared biochars, International Journal of Hydrogen Energy, https://doi.org/10.1016/j.ijhydene.2020.11.230

catalyst in molten eutectic carbonate salt. Int J Hydrogen Energy 2015;40:11809–22. https://doi.org/10.1016/j.ijhydene.2015.06.059.
[65] Yao X, Yu Q, Han Z, Xie H, Duan W, Qin Q. Kinetics of CO_2 gasification of biomass char in granulated blast furnace slag. Int J Hydrogen Energy 2018;43:12002–12. https://doi.org/10.1016/j.ijhydene.2018.04.102.
[66] Wang L, Alsaker N, Skreiberg O, Hovd B. Effect of carbonization conditions on CO_2 gasification reactivity of biocarbon. Energy Procedia 2017;142:932–7. https://doi.org/10.1016/j.egypro.2017.12.149.
[67] Liu Z, Zhang F, Liu H, Ba F, Yan S, Hu J. Pyrolysis/gasification of pine sawdust biomass briquettes under carbon dioxide atmosphere: study on carbon dioxide reduction (utilization) and biochar briquettes physicochemical properties. Bioresour Technol 2018;249:983–91. https://doi.org/10.1016/j.biortech.2017.11.012.
[68] Guizani C, Escudero Sanz FJ, Salvador S. Effects of CO_2 on biomass fast pyrolysis: reaction rate, gas yields and char reactive properties. Fuel 2014;116:310–20. https://doi.org/10.1016/j.fuel.2013.07.101.
[69] Kwon EE, Jeon YJ, Yi H. New candidate for biofuel feedstock beyond terrestrial biomass for thermo-chemical process (pyrolysis/gasification) enhanced by carbon dioxide (CO_2). Bioresour Technol 2012;123:673–7. https://doi.org/10.1016/j.biortech.2012.07.035.
[70] Kwon EE, Yi H, Castaldi MJ. Utilizing carbon dioxide as a reaction medium to mitigate production of polycyclic aromatic hydrocarbons from the thermal decomposition of styrene butadiene rubber. Environ Sci Technol 2012;46:10752–7. https://doi.org/10.1021/es301933p.
[71] Wei L, Xu S, Zhang L, Liu C, Zhu H, Liu S. Steam gasification of biomass for hydrogen-rich gas in a free-fall reactor. Int J Hydrogen Energy 2007;32:24–31. https://doi.org/10.1016/j.ijhydene.2006.06.002.
[72] Mahishi MR, Goswami DY. An experimental study of hydrogen production by gasification of biomass in the presence of a CO_2 sorbent. Int J Hydrogen Energy 2007;32:2803–8. https://doi.org/10.1016/j.ijhydene.2007.03.030.
[73] Ma Z, Zhang SP, Xie DY, Yan YJ. A novel integrated process for hydrogen production from biomass. Int J Hydrogen Energy 2014;39:1274–9. https://doi.org/10.1016/j.ijhydene.2013.10.146.
[74] Cabuk B, Duman G, Yanik J, Olgun H. Effect of fuel blend composition on hydrogen yield in co-gasification of coal and non-woody biomass. Int J Hydrogen Energy 2019;45:3435–43. https://doi.org/10.1016/j.ijhydene.2019.02.130.
[75] Emami Taba L, Irfan MF, Wan Daud WAM, Chakrabarti MH. The effect of temperature on various parameters in coal, biomass and CO-gasification: a review. Renew Sustain Energy Rev 2012;16:5584–96. https://doi.org/10.1016/j.rser.2012.06.015.
[76] Göransson K, Söderlind U, He J, Zhang W. Review of syngas production via biomass DFBGs. Renew Sustain Energy Rev 2011;15:482–92. https://doi.org/10.1016/j.rser.2010.09.032.
[77] Qin K, Lin W, Jensen PA, Jensen AD. High-temperature entrained flow gasification of biomass. Fuel 2012;93:589–600. https://doi.org/10.1016/j.fuel.2011.10.063.
[78] Haryanto A, Fernando SD, Pordesimo LO, Adhikari S. Upgrading of syngas derived from biomass gasification: a thermodynamic analysis. Biomass Bioenergy 2009;33:882–9. https://doi.org/10.1016/j.biombioe.2009.01.010.
[79] Wang L, Alsaker N, Skreiberg O, Hovd B. Effect of carbonization conditions on CO_2 gasification reactivity of biocarbon. Energy Procedia 2017;142:932–7. https://doi.org/10.1016/j.egypro.2017.12.149.
[80] Xiao R, Chen X, Wang F, Yu G. Pyrolysis pretreatment of biomass for entrained-flow gasification. Appl Energy 2010;87:149–55. https://doi.org/10.1016/j.apenergy.2009.06.025.
[81] Ren S, Lei H, Wang L, Bu Q, Chen S, Wu J, et al. The effects of torrefaction on compositions of bio-oil and syngas from biomass pyrolysis by microwave heating. Bioresour Technol 2013;135:659–64. https://doi.org/10.1016/j.biortech.2012.06.091.
[82] Franco C, Pinto F, Gulyurtlu I, Cabrita I. The study of reactions influencing the biomass steam gasification process. Fuel 2003;82:835–42. https://doi.org/10.1016/S0016-2361(02)00313-7.

Please cite this article as: Lampropoulos A et al., Effect of Olive Kernel thermal treatment (torrefaction *vs.* slow pyrolysis) on the physicochemical characteristics and the CO_2 or H_2O gasification performance of as-prepared biochars, International Journal of Hydrogen Energy, https://doi.org/10.1016/j.ijhydene.2020.11.230